Published in final edited form as:
Anal Chem. 2011 May 1; 83(9): 3563–3571. doi:10.1021/ac200143v.

Higher Sensitivity Dopamine Measurements with Faster-Scan Cyclic Voltammetry

Richard B. Keithley[a], **Pavel Takmakov**[a], **Elizabeth S. Bucher**[a], **Anna M. Belle**[a], **Catarina A. Owesson-White**[a], **Jinwoo Park**[a], and **R. Mark Wightman**[a,b,*]

[a] Department of Chemistry, University of North Carolina at Chapel Hill, Chapel Hill, NC 27599, United States

[b] Neuroscience Center and Neurobiology Curriculum, University of North Carolina at Chapel Hill, Chapel Hill, NC 27599, United States

Abstract

Fast-scan cyclic voltammetry with carbon-fiber microelectrodes has been successfully used to detect catecholamine release in vivo. Generally, waveforms with anodic voltage limits of 1.0 V or 1.3 V (vs. Ag/AgCl) are used for detection. The 1.0 V excursion provides good temporal resolution, but suffers from a lack of sensitivity. The 1.3 V excursion increases sensitivity, but also increases response time which can blur the detection of neurochemical events. Here, the scan rate was increased to improve the sensitivity of the 1.0 V excursion while maintaining the rapid temporal response. However, increasing scan rate increases both the desired faradaic current response and the already large charging current associated with the voltage sweep. Analog background subtraction was used to prevent the analog-to-digital converter from saturating from the high currents generated with increasing scan rate by neutralizing some of the charging current. In vitro results with the 1.0 V waveform showed approximately a four-fold increase in signal to noise ratio with maintenance of the desired faster response time by increasing scan rate up to 2400 V/s. In vivo, stable stimulated release was detected with an approximate four-fold increase in peak current. The scan rate of the 1.3 V waveform was also increased, but the signal was unstable with time in vitro and in vivo. Adapting the 1.3 V triangular wave into a sawhorse design prevented signal decay and increased the faradaic response. The use of the 1.3 V sawhorse waveform decreased the detection limit of dopamine with FSCV to 0.96 ± 0.08 nM in vitro and showed improved performance in vivo without affecting the neuronal environment. Electron microscopy showed dopamine sensitivity is in a quasi-steady state with carbon-fiber microelectrodes scanned to potentials above 1.0 V.

Keywords

Fast-scan cyclic voltammetry; carbon-fiber microelectrode; analog background subtraction; dopamine sensitivity; in vivo voltammetry

INTRODUCTION

Fast-scan cyclic voltammetry (FSCV) with carbon-fiber microelectrodes is a useful technique for the in vitro and in vivo detection of various electroactive species including

*To Whom Correspondence Should be Addressed, rmw@email.unc.edu.

SUPPORTING INFORMATION AVAILABLE

Additional information as noted in text. This material is available free of charge via the Internet at http://pubs.acs.org.

catecholamines. FSCV offers many advantages including sub-second time resolution, high spatial resolution, moderate selectivity, and excellent sensitivity.[1] These advantages have allowed users to probe neurochemical signaling dynamics in single cells, adrenal slices, brain slices, and in the intact brains of anesthetized and freely moving rats.[1–3]

Several approaches have been used to improve the signal-to-noise ratios in the detection of neuromodulators with FSCV including improving electrode fabrication[4, 5], signal processing[4, 6], instrumentation[7, 8], and the incorporation of novel electrode coatings.[9, 10] Electrochemical pretreatment also enhances sensitivity towards catecholamines through the creation of adsorption sites.[11–14] Traditional experiments employed FSCV waveforms that had an anodic potential limit of 1.0 V (vs. Ag/AgCl), which provided for good temporal resolution.[14] These waveforms suffered from a lack of sensitivity so waveforms with an anodic limit of 1.3 V are frequently used to provide increased sensitivity in vivo.[15–17] However, the increase in catecholamine adsorption sites associated with higher anodic limits that improve sensitivity increases the response time of the carbon-fiber microelectrode.[14]

Cyclic voltammetry theory predicts that peak current for diffusion-mediated electron transfer varies with the square root of scan rate while peak current for species that adsorb to the electrode surface scales proportionally with scan rate.[18] Catecholamines such as dopamine strongly adsorb to the electrode surface[14, 19, 20] so increasing scan rate proportionally increases their faradaic response. Increasing the scan rate above the traditional[14] 300–400 V/s range is advantageous in the detection of neuromodulators and has been used previously.[19, 21–25]

Unfortunately, charging current also increases proportionally with scan rate.[26] Charging current overwhelms the faradaic signal at the small concentrations of neurotransmitters typically measured, but can be digitally subtracted over short time scales such that only the signal of interest is viewed.[8] However, the large charging current is still measured at the working electrode and leads to numerous disadvantages. First, it can saturate the current-to-voltage converter because of its finite power supply and/or the analog-to-digital converter (ADC) because of its limited voltage range. Also, large charging currents force lower gains to be used which increase quantization error and digitization noise.[27, 28] Dynamically changing the gain requires either the reconfiguration of the current-to-voltage converter or the use of a potentiostat with an adjustable gain, both of which are impractical for experiments in behaving animals.

Recently, analog background subtraction (ABS) was developed in our lab to remove charging current in real time before digitization.[28] In this approach, charging current is recorded and played back at the summing point of the current-to-voltage converter thereby nulling the output in a procedure similar to that of some noise-cancelling headphones. ABS was successfully used to decrease quantization noise and enabled continuous FSCV measurements for up to 30 minutes.

Here, dopamine sensitivity was increased by scanning faster than 400 V/s, but ABS was used to decrease the larger charging currents associated with scanning faster, thereby circumventing the aforementioned disadvantages. One goal was to create a more sensitive 1.0 V excursion while maintaining rapid response time. Another aim was to develop an ultra-sensitive 1.3 V sweep to detect even smaller dopamine signaling events.

EXPERIMENTAL SECTION

Chemicals

Chemicals were purchased from Sigma-Aldrich (St. Louis, MO) and were used as received. Solutions were prepared in doubly distilled deionized water. In vitro experiments were conducted in PBS buffer (10 mM NaH_2PO_4, 140 mM NaCl, 3 mM KCl, adjusted to pH 7.4 with concentrated NaOH). Dopamine stock solutions were prepared in 0.1 N perchloric acid and were diluted with PBS buffer on the day of use. Both the PBS buffer and dopamine solutions were N_2 saturated to prevent oxidative degradation of dopamine over the course of the experiment.

Electrode fabrication

T-650 type (Thornel, Amoco Corporation, Greenville, SC) cylindrical carbon-fiber microelectrodes were fabricated as previously described.[29] The carbon-fibers were cut to a length of 50–75 μm with a scalpel. All electrodes were soaked in isopropanol purified with Norit A activated carbon for at least 20 minutes before use.[19]

Data acquisition

Data was acquired using locally constructed hardware (Carolina Chemistry Electronics Facility) and software in the LabVIEW programming environment (National Instruments, Austin, TX) as described previously.[7, 28] The voltammetric waveform was generated and the data was acquired using a PCI-6052E DAC/ADC card (16 bit, National Instruments). A PCI 6711 card was used for synchronization and flow injection analysis control. Typically, voltammetric waveforms are also low-pass filtered at 2 kHz to remove digitization noise.[30, 31] This filter was unsuitable for the use of faster scan rates and was removed.

Electrochemical experiments

A Ag/AgCl reference electrode was used for all electrochemical experiments. All experiments were performed in a grounded Faraday cage to reduce noise. Several voltage excursions at varying scan rates were used in this work. First, a triangular cyclic sweep from −0.4 V to 1.0 V back to −0.4 V (the “1.0 V waveform”) was used at scan rates varying from 400 V/s to 2400 V/s. Second, a triangular cyclic sweep from −0.4 V to 1.3 V back to −0.4 V (the “1.3 V cyclic waveform”) was used at scan rates of 400 V/s and 2400 V/s. Finally, a voltage excursion was constructed in piecemeal fashion by ramping from −0.4 V to 1.3 V at 2400 V/s, holding at 1.3 V for 0.55 ms, and ramping back to −0.4 V at 2400 V/s. The resulting waveform shape resembled a sawhorse pattern (the “1.3 V sawhorse waveform”, *vide infra*). The number of steps in the voltage waveform was changed with scan rate to maintain the same sampling frequency throughout all experiments. All waveforms used a holding voltage of −0.4 V between voltammetric sweeps.

All experiments began with either the 1.0 V waveform or the 1.3 V cyclic waveform at 400 V/s. Electrodes were cycled with the corresponding waveform for 15 minutes at 60 Hz and 10 Hz for 15 minutes before use. Afterwards, experiments were conducted with a waveform application frequency of 10 Hz. In vitro experiments were conducted using a flow injection analysis system to expose carbon-fiber microelectrodes to a bolus of analyte.[32] In vivo experiments were performed in male Sprague-Dawley rats (~ 350 g, Charles River, Wilmington, MA) anesthetized with urethane (1.5 g/kg i.p., made in a 50% w/w solution of saline) as described previously.[28] Holes were drilled for the carbon-fiber microelectrode in the striatum (+1.3 A/P, +2.3 M/L, −4.0 to −7.5 D/V, in mm relative to bregma), a stimulating electrode in the ventral tegmental area (−5.2 A/P, +1.0 M/L, −7.0 to −9.0 D/V), and a reference placed contralateral to the carbon-fiber microelectrode. A bipolar stimulating electrode was used (Plastics One, Roanoke, VA). Biphasic stimulations (300 μA,

60 Hz, 40 pulses, 2 ms each phase) were delivered using optically isolated constant current stimulators (Digitimer Ltd., Letchworth, UK).

Data analysis

All analyses were conducted using locally written LabVIEW software (National Instruments, Austin, TX), Microsoft Excel (Redmond, WA), and MATLAB (Mathworks, Natick, MA). Statistical tests were performed using GraphPad Prism (GraphPad Software Inc., San Diego, CA). All values and traces are reported as averages ± standard error of the mean. For quantitation of peak currents, noise was removed using only a nearest-neighbor smoothing algorithm as was done previously for faster scan rate experiments.[19] For the calculation of temporal responses, noise was removed solely with a 4^{th} order Bessel low-pass filter. The frequency of the filter in Hz was chosen by multiplying the scan rate by five (ex: 400 V/s filtered at 2 kHz, 800 V/s filtered at 4 kHz, etc.). Response time was quantified to be the amount of time necessary for the peak current to rise from 0% to 90% of its maximum value. The calculation of quantization noise and signal-to-noise ratios is described in Supporting Information.

Etching studies

Scanning electron microscopy was used to study the effect of the applied waveform on the carbon-fiber microelectrode.[31] Carbon-fiber microelectrodes were imaged before and after waveform application in vitro, with the procedure adapted from previous work[31] (detailed in Supporting Information). A one-way ANOVA with Bonferroni's post-test was used to determine significant differences between groups.

Use of ABS for faster scan rate experiments

Figure S-1 shows how ABS was used for faster scan rate experiments. First, charging current was recorded at 400 V/s in the absence of analyte, digitized, and fed into the summing point of the current to voltage converter as a voltage signal.[28] The addition of this signal at the summing point of the current-to-voltage converter will initially yield a zeroed output. Next, the scan rate was increased which results in a larger charging current at the working electrode, but because some of the current can be neutralized, the output voltage will not saturate the ADC. The resulting output was then digitized and digitally background-subtracted[8] to generate analyte cyclic voltammograms and color plots.[33]

Effect of increased charging current on neuronal firing

Combined iontophoresis, ABS, and electrophysiology experiments were performed to study the effect of the increased charging current on local neuronal firing in anesthetized animals. The procedure was adapted from previous work, with filtering and analysis being performed as described elsewhere.[34, 35] A PCI 6040E card was used for electrophysiology recordings and a locally constructed headstage was used that incorporated a solid-state relay that switched between a current-to-voltage converter capable of performing ABS for voltammetric scans and a voltage follower for unit recordings. A multibarrel carbon-fiber microelectrode capable of performing iontophoresis was used for the combined electrochemistry/electrophysiology experiment, whose construction is described elsewhere.[34] The Ag/AgCl electrode served as the reference for both the electrochemical and electrophysiological experiments, as well as the return for the iontophoresis current.

The dorsal-ventral position of the working and stimulating electrodes was optimized to ensure the experiments were performed in an area displaying stimulated dopamine release. Next, a 200 mM L-glutamate solution was locally iontophoresed using a constant current source (15 nA–35 nA, Neurophore, Harvard Apparatus, Holliston, MA) into the

extracellular environment at the carbon-fiber microelectrode tip to evoke firing of medium spiny neurons in the anesthetized animal.[36, 37] Units were then recorded for 10 minutes to ensure a stable baseline.

The waveform application frequency was 5 Hz for these experiments. The duration of the voltammetric scans was 20 ms, which included the voltammetric sweep time and amplifier settling time. The remaining 180 ms was used for unit recording.

RESULTS AND DISCUSSION

Scanning faster with the 1.0 V waveform

Figure 1 shows the effect of increasing scan rate with the 1.0 V waveform. Figure 1A shows normalized peak current versus time traces for a 1 μM dopamine injection in vitro at various scan rates. The rapid response time of the 1.0 V waveform was not significantly different between 400, 800, 1200, 1600, 2000, and 2400 V/s (N = 5 electrodes, P = 0.5113, repeated measures ANOVA), even though peak current increased with scan rate (Figure S-2).

Previous work has shown that a major noise source of FSCV measurements is the finite step size of data quantization.[28] Since gain of the current-to-voltage converter remained unchanged while increasing scan rate in this work, the noise level should remain constant. While quantization noise was independent of scan rate (N = 5 electrodes, P = 0.5707, repeated measures ANOVA), electrode drift increased as the scan rate was increased.

Figure 1B shows the current versus time trace taken at the oxidation potential of dopamine during a stimulated release event in vivo. The measured dopamine current increased throughout the duration of the stimulation and uptake caused the current response to decrease after the stimulation ended as dopamine was removed from the extracellular space. Figure 1C shows cyclic voltammograms measured from ten consecutive stimulated dopamine release events in vivo at 2400 V/s (solid traces), compared to the response measured at 400 V/s (dotted trace) with the 1.0 V waveform.

Increasing the scan rate to 2400 V/s increased the faradaic response, but there was a 190 mV shift in peak potential. This peak shift at high scan rates has been reported before[19, 25] and was likely due to a combination of slow kinetics of dopamine oxidation[38, 39], an increased cell time constant, and ohmic drop[40, 41], both of which are larger for cylindrical microelectrodes[42] compared to disc microelectrodes[43]. The capacitance of the glass coated portion of the carbon-fiber microelectrode present with longer electrode tapers may also play a role.[41] The time constant of the current-to-voltage converter was approximately 2.4 μs which negligibly distorts the measured response.[44] While undesirable, this peak shift did not interfere with dopamine identification but 2400 V/s was chosen as the maximal scan rate to prevent oxidation from occurring past the 1.0 V switching potential.

The stability of the increased faradaic response in vitro and in vivo was examined. Increasing scan rate from 400 V/s to 2400 V/s with the 1.0 V waveform initially gave a 4.8 ± 0.1 fold increase in peak current in vitro that stabilized to a 4.4 ± 0.1 fold increase after approximately 20 minutes (Figure 1D, filled squares, N = 5 electrodes). Dopamine is known to strongly adsorb to the carbon-fiber microelectrode using this waveform because of the negative holding potential and electrostatic effects;[14, 19, 31] therefore, peak current should scale in direct proportion with scan rate. Since the amount of dopamine that is oxidized should remain constant, integral charge should also remain constant. However, the broadening shift of the oxidation peak (Figure 1C) would cause peak current to be smaller than theory predicts to maintain the same overall peak area (Figure S-2). The less than expected fold increase in peak current did not depend on the buffer used, as a 4.3 ± 0.2 fold

increase in peak current was measured in HEPES (20 mM HEPES, 150 mM NaCl, 1.2 mM $CaCl_2$) when scan rate was increased from 400 V/s to 2400 V/s with the 1.0 V waveform which was not significantly different from that measured in PBS (N = 4, P = 0.6875, unpaired t-test).

ABS was originally used to increase signal to noise ratios of electrochemical measurements by decreasing quantization noise.[28] The combination of ABS and increased scan rate was used to increase the signal to noise ratio for 1 μM dopamine approximately 4-fold in vitro from 333 ± 48 at 400 V/s to 1321 ± 187 at 2400 V/s. However, this value is slightly less than expected for the 4.4-fold increase in signal. The addition of the background signal necessary for current subtraction with faster scan rate experiments likely introduces noise into the system. Also, the lack of a ramp filter likely introduces greater noise at higher scan rates.[7] Assuming a limit of detection of three times the standard deviation of the noise (3σ) in the peak current versus time dimension, these signal-to-noise ratios correspond to theoretical limits of detection of 9.7 ± 1.3 nM at 400 V/s to 2.5 ± 0.3 nM at 2400 V/s.

In vivo, a stable 4.1 ± 0.1 fold increase in oxidative peak current of stimulated dopamine release was detected (Figure 1D, open circles, N = 5). The relative standard deviations of stimulated dopamine release oxidative peak currents at 400 V/s and 2400 V/s were 2.9 ± 0.4% and 4.3 ± 1.0%, respectively and were not significantly different (N = 5, P = 0.1958, paired t-test). Taken together, these results show the desired temporal response of the 1.0 V waveform is maintained at higher scan rates and dopamine release in vivo remained stable with higher scan rates with the 1.0 V waveform.

Scanning faster with the 1.3 V cyclic waveform

The scan rate of the 1.3 V cyclic waveform was increased to create an ultra-sensitive voltage sweep. Figure 2 shows the effect of increasing scan rate with the 1.3 V cyclic waveform. Unlike the 1.0 V waveform, the 1.3 V cyclic waveform showed an unstable increase in peak current both in vitro and in vivo, as shown in Figure 2A. Figure 2B shows in vivo cyclic voltammograms of ten consecutive stimulated dopamine release events measured at 2400 V/s with the 1.3 V cyclic waveform every four minutes (solid lines). Again, a peak shift was apparent compared to the cyclic voltammogram measured at 400 V/s (dashed line).

Figure 2A showed that increasing scan rate 6-fold increased the peak current 7.2 ± 0.1 fold in vitro (N = 5 electrodes). To investigate this, in vitro cyclic voltammograms were integrated to calculate charge as a function of time for the in vitro data shown in Figure 2A with the results plotted in Figure 2C. Ideally, charge should remain constant as scan rate is increased as long as the number of moles of dopamine electrolyzed does not change. Upon switching from 400 V/s to 2400 V/s with the 1.3 V cyclic waveform, there was an initial 53 ± 3% (N = 5 electrodes) increase in charge that quickly decayed over time. When switching back to 400 V/s, there was significantly less charge than there had been during the 400 V/s baseline period, but integral charge returned to baseline after approximately 20 minutes.

Only an increase in electrode area and/or adsorbed species would result in a higher than expected peak current for adsorption-mediated electron transfer.[18] While the 1.3 V cyclic waveform is known to oxidatively etch carbon-fiber surfaces, it is unlikely that electrode area changed in such an erratic manner so quickly because the oxidative etch is mild compared to other voltammetric excursions which are known to fracture carbon surfaces.[31] Instead, this result suggests that the amount of dopamine adsorbed on the carbon-fiber microelectrode surface increased upon increasing scan rate. In other words, surface chemistry rather than surface structure likely changes, as hypothesized previously.[11]

The duration of the 1.3 V cyclic waveform at 400 V/s is 8.5 ms, compared to 1.4 ms at 2400 V/s, so some of the increased adsorption could be due to an increased holding time. Taking into account that dopamine can still adsorb during the voltage sweep before its oxidation,[19] the holding time at 2400 V/s is equivalent to an application frequency of 9.4 Hz at 400 V/s with the 1.3 V cyclic waveform. Charge did not significantly change with this longer holding time at 400 V/s ($N = 3$, $P = 0.9015$, paired t-test) so the increase in charge seen at 2400 V/s with the 1.3 V cyclic waveform was due to an increase in adsorption site availability.

While the exact potential necessary to oxidatively etch the carbon-fiber surface for enhanced sensitivity is unknown, each 1.3 V cyclic sweep at 400 V/s spends approximately 1.5 ms above 1.0 V as shown in Figure S-3A. Increasing scan rate to 2400 V/s decreases this time by 6 to approximately 250 μs (Figure S-3B). We previously hypothesized that adsorption sites are consumed with a Kolbe-like electrolysis that occurs at potentials above 1.0 V.[31] Decreasing the amount of time at potentials above 1.0 V would also prevent adsorption site degradation, thereby increasing the number of available sites for dopamine adsorption which could explain the increase in measured charge. If an oxidative etching mechanism maintains adsorption sites necessary for dopamine sensitivity, scanning faster would decrease the amount of time spent at potentials necessary for this process to occur. As time progresses, sensitivity could decrease as adsorption sites foul, possibly due to irreversible adsorption of impurities or oxidative byproducts.[31]

Supporting this hypothesis, Hafizi et al. described decreasing sensitivity with time as the anodic voltage limit of the applied waveform was switched from 1.4 V to 1.0 V.[11] Specifically, they describe a “semi-reversible change in the electrode surface”, which likely also explains the return to baseline behavior seen in Figure 2C after switching back to 400 V/s from 2400 V/s. The authors go on to state that continual application of the 1.4 V waveform was necessary for maintenance of enhanced sensitivity with time.

Interestingly, switching from 400 V/s to 2400 V/s also decreased the response time of the 1.3 V cyclic waveform by 60 ± 5% ($N = 5$) as shown in Figure 2D. This decreased response time occurred even though more material was adsorbed on the carbon-fiber microelectrode surface (Figure 2C). If the amount of time spent at potentials above 1.0 V becomes insufficient for surface activation, the temporal response of the 1.3 V cyclic waveform at 2400 V/s may become similar to that seen with the 1.0 V waveform. Taken together, these data show how scanning to anodic potentials higher than 1.0 V on carbon-fiber microelectrodes creates a quasi-steady state electrochemical surface.

Modification of the 1.3 V cyclic waveform for maintaining increased sensitivity

The 1.3 V cyclic waveform was adapted to correct the unstable loss in sensitivity over time. To increase the sensitivity, the scan rate was increased from 400 V/s to 2400 V/s. An anodic holding time was added at the switching potential between the anodic and cathodic voltage sweeps to create a 1.3 V sawhorse-shaped waveform as shown in Figure S-3C. For a stable response, the ideal anodic holding time between the oxidative and reductive sweeps was 0.55 ms for a total waveform length of 1.97 ms. If the anodic holding time was less than 0.55 ms, the performance mimicked the response seen in Figure 2A. If the anodic holding time was greater than 0.55 ms, the opposite trend was seen with an unstable increase in dopamine sensitivity (data not shown).

Figure 3 shows the in vitro performance of the 1.3 V sawhorse waveform. A representative cyclic voltammogram for 1 μM dopamine with the 1.3 V sawhorse waveform at 2400 V/s is shown in Figure 3A (solid trace) with the response towards dopamine at 400 V/s with the 1.3 V cyclic waveform with the same electrode is also shown (dashed trace) for comparison.

The response time of the 1.3 V sawhorse waveform at 2400 V/s also decreased by 26 ± 6% (N = 5 electrodes) as shown in Figure 3B.

The 1.3 V sawhorse waveform at 2400 V/s corrected the instability measured with the 1.3 V cyclic waveform at 2400 V/s (Figure 3C, N = 5 electrodes). The application of the 1.3 V sawhorse waveform at 2400 V/s also significantly increased voltammetric noise by 7.9 ± 1.8%, which remained elevated even after switching back to the 1.3 V cyclic waveform at 400 V/s (N = 5, P = 0.0015, repeated measures ANOVA). In all, the signal-to-noise ratio for 1 μM dopamine increased from 602 ± 73 to 3322 ± 311 when switching from the 1.3 V cyclic waveform at 400 V/s to the 1.3 V sawhorse waveform at 2400 V/s, respectively. Assuming a limit of detection of 3σ, these signal to noise ratios correspond to a lowering of the theoretical limits of detection from 5.3 ± 0.7 nM to 0.96 ± 0.08 nM when switching from the 1.3 V cyclic waveform at 400 V/s to the 1.3 V sawhorse waveform at 2400 V/s, respectively.

Integrating oxidative peak current showed that upon switching to the 1.3 V sawhorse waveform at 2400 V/s, charge initially increased 39 ± 2% in vitro and showed a stable level of adsorption throughout the period of waveform application. Again, it is unlikely that electrode area would show such a rapid increase, only to return to baseline when switching back to the 1.3 V cyclic waveform at 400 V/s. Instead, it is more likely that the application of the 1.3 V sawhorse waveform at 2400 V/s increased the amount of material adsorbed to the carbon-fiber microelectrode surface. Interestingly, the response time decreased in vitro (Figure 3B) despite having more material adsorbed. This implies that the 1.3 V sawhorse waveform at 2400 V/s, the 1.3 V cyclic waveforms at 400 V/s and 2400 V/s, and the 1.0 V waveform at all scan rates had distinct surface chemistries that adsorbed dopamine differently in vitro.

The performance of the 1.3 V sawhorse waveform at 2400 V/s in vivo is shown in Figure 4. Representative color plots show that the measured faradaic response increased (Figures 4A and 4B). Overall, there was a stable 4.3 ± 0.3 fold increase in peak current of stimulated dopamine release (N = 8 locations in seven rats), similar to that seen with the 1.0 V waveform at 2400 V/s (Figure 1D). One animal showed over a 40% decrease in peak current after switching to the 1.3 V sawhorse waveform at 2400 V/s and these data were discarded. The average relative standard deviation of stimulated dopamine release peak currents significantly increased from 2.5 ± 0.3 % with the 1.3 V cyclic waveform at 400 V/s to 5.6 ± 1.0% with the 1.3 V sawhorse waveform at 2400 V/s (N = 8, P = 0.0468, paired t-test) but was still small overall and was well within the known stability of stimulated dopamine release over time.[45] Integrating oxidative peak current showed that, except for the stimulated release events immediately following the switches in waveforms, charge remained constant throughout the course of the in vivo experiment (Figure 4D).

Effect of increased charging currents on local neuronal activity in vivo

A combined electrochemistry and electrophysiology experiment[35, 46] was performed to examine if the large charging currents generated by the 1.3 V sawhorse waveform at 2400 V/s effects local cell firing in vivo. With the exception of chronoamperometry with larger electrodes,[47] previous work has shown that currents associated with electrochemical measurements performed with microelectrodes are too small to impact neuronal firing.[48–51] However, the charging currents generated at the working electrode by scanning faster are larger (typically between 2.5 μA to 3.5 μA for the 1.3 V sawhorse waveform at 2400 V/s).

The firing rate of neurons in anesthetized animals is generally low so glutamate was locally delivered in vivo to evoke cell firing.[36, 37] A multibarrel iontophoresis probe[34] was used to

deliver glutamate to the same local area in which the charging current was generated and the electrophysiological recordings were made.

Figure 5 shows the effect of increased charging current on glutamate-evoked cell firing (N = 21 cells in 4 rats). The iontophoresis probe evoked cell firing of striatal neurons in the anesthetized animal while simultaneously measuring their firing pattern, as well as performing a voltammetric measurement. The 1.3 V sawhorse waveform at 2400 V/s did not significantly affect the average glutamate-evoked firing rate of medium spiny neurons in vivo ($P = 0.7713$, repeated measures ANOVA). Since the 1.3 V sawhorse waveform at 2400 V/s had the largest charging current of any of the voltage excursions studied, scanning faster with all other waveforms also should not affect the local cellular environment.

Surface integrity of carbon-fiber microelectrodes after waveform application

Recently, we have demonstrated the use of environmental scanning electron microscopy (ESEM) as a way to monitor etching that occurs upon waveform application.[31] Unlike traditional scanning electron microscopy, the samples to be imaged do not need to be coated with a conductor in ESEM. Any change in carbon-fiber diameter can be quantified and a linear etch rate with respect to the number of waveform cycles applied can be determined.

Figure S-4 and Figure 6 show the effect of each waveform on the etching of carbon-fiber microelectrodes. Figure S-4 shows representative images of carbon-fiber microelectrodes after the application of each waveform. Figure 6 shows that the waveform applied significantly affected the etching rate of the carbon-fiber microelectrode ($N = 5$ each, $P < 0.0001$, one-way ANOVA). As shown previously,[31] application of the 1.0 V waveform at 400 V/s did not significantly etch the carbon-fiber microelectrode (Figure 6-I). Increasing the scan rate to 2400 V/s with the 1.0 V waveform also did not significantly etch the microelectrode (Figure 6-II). This result confirms earlier observations from Figure 1 regarding the stable increase in signal, maintenance of time response, and similar voltammetric noise levels when increasing scan rate of the 1.0 V waveform.

The 1.3 V cyclic waveform at 400 V/s etched the surface as shown before[31] (Figure 6-III), but increasing the scan rate of this waveform to 2400 V/s significantly decreased the etch rate (Figure 6-IV) to a value comparable to that of the 1.0 V excursions. This comparable etch rate probably contributes to the decreased time response and loss in sensitivity with the 1.3 V cyclic waveform at 2400 V/s.

The 1.3 V sawhorse waveform at 2400 V/s had the largest etch rate of any waveform evaluated (Figure 6-V), etching significantly more than the 1.3 V cyclic waveform at 400 V/s and 2400 V/s. It is interesting that more etching was needed than the 1.3 V cyclic waveform at 400 V/s to maintain sensitivity over time. An increased etching rate, yet faster time response suggests that the adsorption sites created with the 1.3 V sawhorse waveform at 2400 V/s differ from those present with the 1.3 V cyclic excursions. The increase in electrode noise measured with the 1.3 V sawhorse waveform at 2400 V/s, that is still present upon switching back to the 1.3 V cyclic waveform at 400 V/s, was likely due to either a more reactive electrode etching process, sub-micron electrode resurfacing not visible with the ESEM, or a deterioration of the electrode-glass seal as more of the carbon-fiber microelectrode is etched. Taken together, the in vitro responses and etching data shows that while the 1.3 V sawhorse waveform at 2400 V/s maintains sensitivity over time, it does not maintain the same surface structure and chemistry.

CONCLUSION

This work demonstrates the use of faster than the traditional scan rates for enhanced in vivo sensitivity towards dopamine without increasing quantization error. Signal to noise ratios increased approximately 4-fold upon increasing scan rate from 400 V/s to 2400 V/s with the 1.0 V waveform. The temporal response and stability of measured dopamine release was unaffected by increasing scan rate with this waveform. However, increasing the scan rate from 400 V/s to 2400 V/s led to an unstable decrease in sensitivity in vitro and in vivo with the 1.3 V cyclic waveform. The creation of a novel sawhorse waveform corrected this loss in sensitivity, but did not maintain the same surface chemistry as the 1.3 V cyclic waveform at 400 V/s.

A prime advantage in focusing on increasing sensitivity is that other methods of noise reduction referenced in the introduction can be combined with this approach for even higher signal to noise ratios. This initial characterization necessitates several future experiments. This work could be extended to measurements in freely-moving rats performing behavioral tasks, where localized pH changes are also routinely measured.[52, 53] Norepinephrine and serotonin are present in low levels so their detection would be facilitated by improved sensitivity.[22, 54]

Supplementary Material

Refer to Web version on PubMed Central for supplementary material.

Acknowledgments

The authors acknowledge financial support from NIH (DA 10900) and a National Defense Science and Engineering Graduate Fellowship for R.B.K. The authors thank the Carolina Chemistry Electronics Facility and Collin J. McKinney for their work in hardware construction and helpful conversations.

References

1. Robinson, DL.; Wightman, RM. Electrochemical Methods for Neuroscience. Michael, AC.; Borland, LM., editors. CRC Press; Boca Raton, FL: 2007. p. 17-36.
2. Ge S, Koseoglu S, Haynes C. Anal Bioanal Chem. 2010; 397:3281–3304. [PubMed: 20521141]
3. Petrovic J, Walsh PL, Thornley KT, Miller CE, Wightman RM. Endocrinology. 2010; 151:1773–1783. [PubMed: 20181796]
4. Rice ME, Nicholson C. Anal Chem. 1989; 61:1805–1810. [PubMed: 2802146]
5. Strand AM, Venton BJ. Anal Chem. 2008; 80:3708–3715. [PubMed: 18416534]
6. Wiedemann DJ, Kawagoe KT, Kennedy RT, Ciolkowski EL, Wightman RM. Anal Chem. 1991; 63:2965–2970. [PubMed: 1789456]
7. Michael DJ, Joseph JD, Kilpatrick MR, Travis ER, Wightman RM. Analytical Chemistry. 1999; 71:3941–3947. [PubMed: 10500480]
8. Howell JO, Kuhr WG, Ensman RE, Wightman RM. J Electroanal Chem. 1986; 209:77–90.
9. Kawagoe KT, Wightman RM. Talanta. 1994; 41:865–874. [PubMed: 18966011]
10. Swamy BEK, Venton BJ. Analyst. 2007; 132:876–884. [PubMed: 17710262]
11. Hafizi S, Kruk ZL, Stamford JA. J Neurosci Meth. 1990; 33:41–49.
12. Gonon FG, Fombarlet CM, Buda MJ, Pujol JF. Anal Chem. 1981; 53:1386–1389.
13. Gonon F, Buda M, Cespuglio R, Jouvet M, Pujol JF. Nature. 1980; 286:902–904. [PubMed: 7412872]
14. Heien ML, Phillips PE, Stuber GD, Seipel AT, Wightman RM. Analyst. 2003; 128:1413–1419. [PubMed: 14737224]

15. Roitman MF, Wheeler RA, Wightman RM, Carelli RM. Nat Neurosci. 2008; 11:1376–1377. [PubMed: 18978779]
16. Gan JO, Walton ME, Phillips PEM. Nat Neurosci. 2010; 13:25–27. [PubMed: 19904261]
17. Day JJ, Roitman MF, Wightman RM, Carelli RM. Nat Neurosci. 2007; 10:1020–1028. [PubMed: 17603481]
18. Bard, AJ.; Faulkner, LR. Electrochemical Methods: Fundamentals and Applications. 2. John Wiley & Sons, Inc; New York: 2001.
19. Bath BD, Michael DJ, Trafton BJ, Joseph JD, Runnels PL, Wightman RM. Analytical Chemistry. 2000; 72:5994–6002. [PubMed: 11140768]
20. Baur JE, Kristensen EW, May LJ, Wiedemann DJ, Wightman RM. Anal Chem. 1988; 60:1268–1272. [PubMed: 3213946]
21. Jackson BP, Dietz SM, Wightman RM. Anal Chem. 1995; 67:1115–1120. [PubMed: 7717525]
22. Hashemi P, Dankoski EC, Petrovic J, Keithley RB, Wightman RM. Anal Chem. 2009; 81:9462–9471. [PubMed: 19827792]
23. Pihel K, Schroeder TJ, Wightman RM. Anal Chem. 1994; 66:4532–4537.
24. Troyer KP, Wightman RM. J Biol Chem. 2002; 277:29101–29107. [PubMed: 12034731]
25. Hsueh C, Bravo R, Jaramillo AJ, Brajter-Toth A. Anal Chim Acta. 1997; 349:67–76.
26. Michael, AC.; Wightman, RM. Laboratory Techniques in Electroanalytical Chemistry. Kissinger, PT.; Heineman, WR., editors. Marcel Dekker, Inc; New York: 1996. p. 367-402.
27. Cahill PS, Walker QD, Finnegan JM, Mickelson GE, Travis ER, Wightman RM. Anal Chem. 1996; 68:3180–3186. [PubMed: 8797378]
28. Hermans A, Keithley RB, Kita JM, Sombers LA, Wightman RM. Anal Chem. 2008; 80:4040–4048. [PubMed: 18433146]
29. Cahill PS, Walker QD, Finnegan JM, Mickelson GE, Travis ER, Wightman RM. Anal Chem. 1996; 68:3180–3186. [PubMed: 8797378]
30. Heien ML, Phillips PE, Stuber GD, Seipel AT, Wightman RM. Analyst. 2003; 128:1413–1419. [PubMed: 14737224]
31. Takmakov P, Zachek MK, Keithley RB, Walsh PL, Donley C, McCarty GS, Wightman RM. Anal Chem. 2010; 82:2020–2028. [PubMed: 20146453]
32. Kristensen EW, Wilson RL, Wightman RM. Anal Chem. 1986; 58:986–988.
33. Michael D, Travis ER, Wightman RM. Anal Chem. 1998; 70:586a–592a.
34. Herr NR, Kile BM, Carelli RM, Wightman RM. Anal Chem. 2008; 80:8635–8641. [PubMed: 18947198]
35. Owesson-White CA, Ariansen J, Stuber GD, Cleaveland NA, Cheer JF, Wightman RM, Carelli RM. Eur J Neurosci. 2009; 30:1117–1127. [PubMed: 19735286]
36. White SR, Harris GC, Imel KM, Wheaton MJ. Brain Res. 1995; 681:167–176. [PubMed: 7552276]
37. Hu XT, White FJ. Neurosci Lett. 1997; 224:61–65. [PubMed: 9132692]
38. Deakin MR, Kovach PM, Stutts KJ, Wightman RM. Anal Chem. 1986; 58:1474–1480. [PubMed: 3728997]
39. Deakin MR, Wightman RM. J Electroanal Chem. 1986; 206:167–177.
40. Wightman RM, Wipf DO. Accounts Chem Res. 1990; 23:64–70.
41. Wipf DO, Michael AC, Wightman RM. J Electroanal Chem. 1989; 269:15–25.
42. Robinson RS, Mccurdy CW, Mccreery RL. Anal Chem. 1982; 54:2356–2361.
43. Wightman, RM.; Wipf, DO. Electroanalytical Chemistry: A Series of Advances. Bard, AJ., editor. Vol. 15. Marcel Dekker; New York, NY: 1989. p. 221-374.
44. Wipf DO, Kristensen EW, Deakin MR, Wightman RM. Anal Chem. 1988; 60:306–310.
45. Ewing AG, Bigelow JC, Wightman RM. Science. 1983; 221:169–171. [PubMed: 6857277]
46. Cheer JF, Heien MLAV, Garris PA, Carelli RM, Wightman RM. Proc Natl Acad Sci U S A. 2005; 102:19150–19155. [PubMed: 16380429]
47. Hefti F, Felix D. J Neurosci Meth. 1983; 7:151–156.

48. Armstrong-James, M.; Millar, J. Measurement of neurotransmitter release in vivo. Marsden, CA., editor. Wiley; Chichester [West Sussex]; New York: 1984. p. 209-224.
49. Stamford JA, Palij P, Davidson C, Jorm CM, Millar J. J Neurosci Meth. 1993; 50:279–290.
50. Ewing AG, Alloway KD, Curtis SD, Dayton MA, Wightman RM, Rebec GV. Brain Res. 1983; 261:101–108. [PubMed: 6301620]
51. Johnson MD, Franklin RK, Gibson MD, Brown RB, Kipke DR. J Neurosci Meth. 2008; 174:62–70.
52. Heien M, Khan AS, Ariansen JL, Cheer JF, Phillips PEM, Wassum KM, Wightman RM. Proc Natl Acad Sci U S A. 2005; 102:10023–10028. [PubMed: 16006505]
53. Takmakov P, Zachek MK, Keithley RB, Bucher ES, McCarty GS, Wightman RM. Anal Chem. 2010; 82:9892–9900. [PubMed: 21047096]
54. Park J, Kile BM, Wightman RM. Eur J Neurosci. 2009; 30:2121–2133. [PubMed: 20128849]

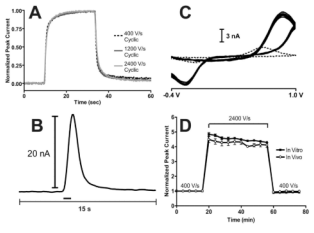

Figure 1.

Performance characteristics of the 1.0 V waveform upon increasing scan rate. A) Temporal response for in vitro injections of 1 μM dopamine at 400 V/s (black dashed line), 1200 V/s (dark grey solid line), and 2400 V/s (light grey solid line) for a representative electrode. B) Current versus time trace at the oxidation potential of dopamine for a representative stimulation in an anesthetized rat. The black bar indicates the duration of the stimulus. C) Cyclic voltammograms from ten consecutive stimulated dopamine release events measured in vivo at 2400 V/s (solid lines) from a representative animal. The dotted line represents the cyclic voltammogram of dopamine at 400 V/s for comparison. D) Baseline normalized dopamine peak current as a function of time for the 1.0 V waveform at 400 V/s, 2400 V/s, and back to 400 V/s in vitro (filled squares) and in vivo (open circles). In vitro peak currents were measured from 1 μM dopamine injections (N = 5 electrodes) and in vivo responses were measured from stimulated dopamine release in anesthetized rats (N = 5 rats). Both responses were measured every four minutes.

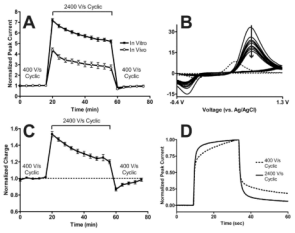

Figure 2.

Performance characteristics of the 1.3 V cyclic waveform upon increasing scan rate. A) Baseline normalized dopamine peak current as a function of time for the 1.3 V cyclic waveform at 400 V/s, 2400 V/s, and back to 400 V/s in vitro (filled squares) and in vivo (open circles). In vitro peak currents were measured from 1 μM dopamine injections (N = 5 electrodes) and in vivo responses were measured from stimulated dopamine release in anesthetized rats (N = 5 rats). Both responses were measured every four minutes. B) Cyclic voltammograms from ten consecutive stimulated dopamine release events measured in vivo at 2400 V/s (solid lines) from a representative animal. The arrow indicates time progression. The dotted line represents the cyclic voltammogram of dopamine at 400 V/s for comparison. C) Baseline normalized charge for the in vitro data shown in A). D) Temporal response for in vitro injections of 1 μM dopamine at 400 V/s (black dashed line) and 2400 V/s (black solid line).

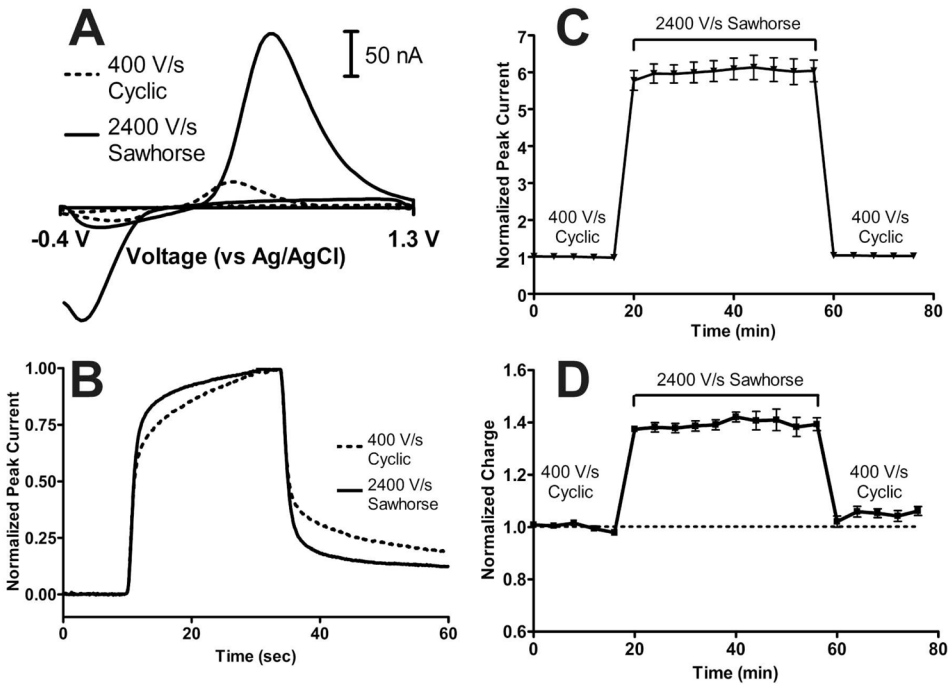

Figure 3.

In vitro performance of the 1.3 V sawhorse waveform. A) Representative cyclic voltammograms for the 1.3 V cyclic waveform at 400 V/s (dashed trace) and the 1.3 V sawhorse waveform at 2400 V/s (solid trace). B) Temporal response for in vitro injections of 1 μM dopamine at 400 V/s with the 1.3 V cyclic waveform (black dashed line) and at 2400 V/s with the 1.3 V sawhorse waveform (black solid line). C) Baseline normalized dopamine peak current as a function of time for the 1.3 V cyclic waveform at 400 V/s, the 1.3 V sawhorse waveform at 2400 V/s, and back to the 1.3 V cyclic waveform at 400 V/s in vitro. In vitro peak currents were measured from 1 μM dopamine injections measured every four minutes (N = 5 electrodes). D) Baseline normalized charge for the in vitro data shown in C).

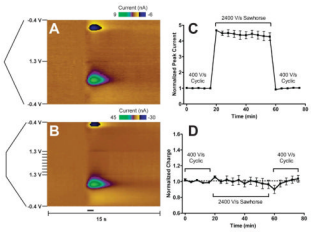

Figure 4.

In vivo performance of the 1.3 V sawhorse waveform in vivo in anesthetized rats. A) Color plot representation of stimulated dopamine release with the 1.3 V cyclic waveform at 400 V/s. B) Color plot representation of stimulated dopamine release with the 1.3 V sawhorse waveform at 2400 V/s. Both A) and B) have the voltammetric sweep plotted to the left of the color plot and the time axis plotted below B). The black bar indicates the duration of the stimulus. C) Baseline normalized dopamine peak current as a function of time for the 1.3 V cyclic waveform at 400 V/s, the 1.3 V sawhorse waveform at 2400 V/s, and back to the 1.3 V cyclic waveform at 400 V/s in vivo (N = 8 locations in seven rats). D) Baseline normalized charge for the in vivo data shown in C).

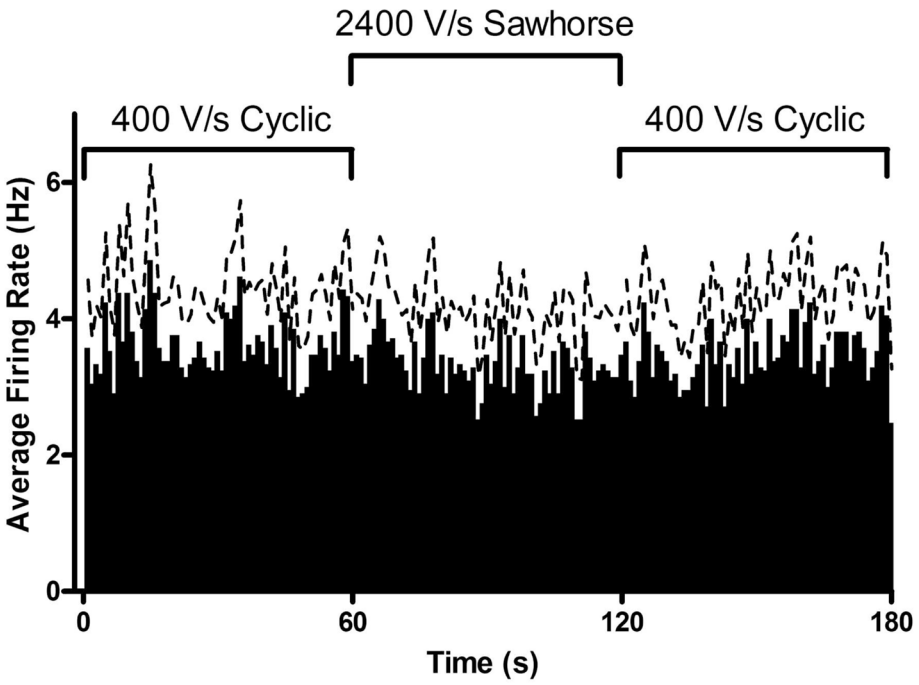

Figure 5.

Average glutamate-evoked firing rate of striatal neurons as a function of time for the 1.3 V cyclic waveform at 400 V/s, the 1.3 V sawhorse waveform at 2400 V/s, and back to the 1.3 V cyclic waveform at 400 V/s (N = 21 cells in 4 rats). The dashed line represents standard error of the mean.

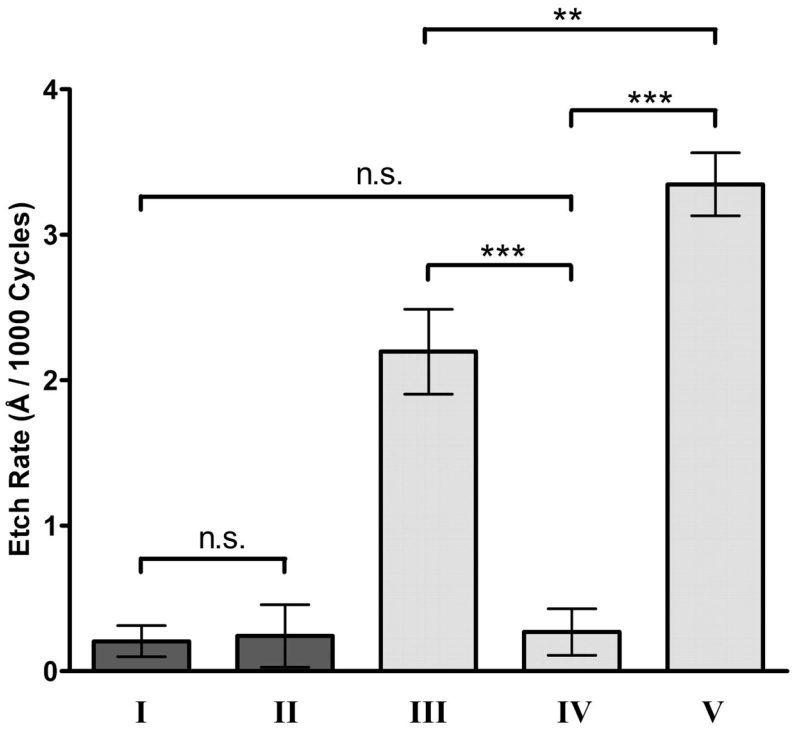

Figure 6.

Carbon-fiber microelectrode etching as a function of the applied waveform. Etch rates for (I) the 1.0 V waveform at 400 V/s, (II) the 1.0 V waveform at 2400 V/s, (III) the 1.3 V cyclic waveform at 400 V/s, (IV) the 1.3 V cyclic waveform at 2400 V/s, and (V) the 1.3 V sawhorse waveform at 2400 V/s. Etch rates are quantified as Angstroms per one thousand waveform applications. N = 5 electrodes for each condition. Only selected comparisons are shown for clarity (n.s. – no significant difference, ** - $P < 0.01$, *** - $P < 0.001$).